PACS numbers: 73.90._f, 81.05.Dz

STUDIES ON METAL-OXIDE SEMICONDUCTOR ZnO AS A HYDROGEN GAS SENSOR

C.S. Prajapati, P.P. Sahay

Department of Physics, Motilal Nehru National Institute of Technology, Allahabad-211 004, India
E-mail: dr_ppsahay@rediffmail.com

Metal-oxide semiconductor ZnO *thin films were prepared on glass slides by spray pyrolysis technique at substrate temperature (410 ± 10) °C.* $Zn(NO_3)_2.6H_2O$ *was used as the precursor solution. The films thus prepared are undergone for structural and morphological studies using X-ray diffraction and scanning electron microscopy The films are found to be polycrystalline zinc oxide in nature, possessing hexagonal wurtzite crystal structure and nanocrystalline in grain size ~* 30-35 *nm. The hydrogen sensing performance of the films has been investigated for various concentration of hydrogen in air at different operating temperatures in the range* 200-400 °C. *It is observed that the response is maximum (*44.3 %*) at the operating of temperature of* 250 °C *for* 0.8 *vol % concentration of hydrogen in air. A possible sensing mechanism for hydrogen has been proposed.*

Keywords: *METAL-OXIDE SEMICONDUCTOR, ZINC OXIDE, HYDROGEN GAS SENSOR, STRUCTURAL PROPERTIES, ELECTRICAL PROPERTIES.*

(Received 04 February 2011, in final form 14 October 2011)

1. INTRODUCTION

Zinc oxide **(ZnO)** is one of the most prominent metal-oxide semiconductors. Because of its good electrical and optical properties, thermal/ chemical stability, abundance in nature, low cost and absence of toxicity, this material has got wide applications in electronic and optoelectronic devices such as transparent conductors, solar cell windows, gas sensors, surface acoustic wave **(SAW)** devices, heat mirrors etc. [1-5]. For gas sensor applications, ZnO in thin film form is more suitable because the gas sensing properties are related to the material surface where the gases are adsorbed and the surface reactions occur [6-11]. Because of large surface-to-volume ratio, the nanostructured thin films have drawn considerable attention of researchers these days.

Several deposition techniques have been used to grow ZnO thin films. These include vacuum evaporation, sputtering, pulse laser deposition, sol-gel process, chemical vapour deposition, spray pyrolysis, etc. In the present investigation, the authors have used spray pyrolysis technique to prepare thin films of ZnO, using an aqueous solution of $Zn(NO_3)_2.6H_2O$ as the precursor solution. Here, we report on the details of preparing of ZnO thin films by spray pyrolysis and the sensing behaviour of the films to hydrogen.

2. EXPERIMENTAL DETAILS

The ZnO films were prepared on cleaned glass substrates which were mounted on a steel plate kept on an electric heater. A particular temperature could be achieved by supplying a suitablepower to the heater through a variac. The schematic experimental set-up of the spray pyrolysis technique for ZnO thin film deposition has been described elsewhere [12]. The spraying solution used was of 0.1 M concentration of high purity $Zn(NO_3)_2.6H_2O$ (Merck, India) prepared in distilled water. The solution was sprayed onto the heated substrates using a locally designed glass nozzle. The atomization of the solution into a spray of fine droplets was affected by the spray nozzle with the help of compressed air as carrier gas. During the course of spray, the substrate temperature was monitored using a chromel-alumel thermocouple with the help of a Motwane digital multimeter (Model: DM 3540A), and was maintained at about (410 ± 10) °C.

The thickness of the films was estimated by the weigh-difference method and found to be in the range 300-400 nm. Structural analysis of these films was carried out using a Bruker AXS C-8 advanced diffractometer with CuKα radiation (λ = 1.5406 Å) as an X-ray source at 40 kV and 30mA in the scanning angle (2θ) from 30° to 80° with scan speed 1°/minute. The surface morphology of the films was investigated with a LEO scanning electron microscope (SEM).
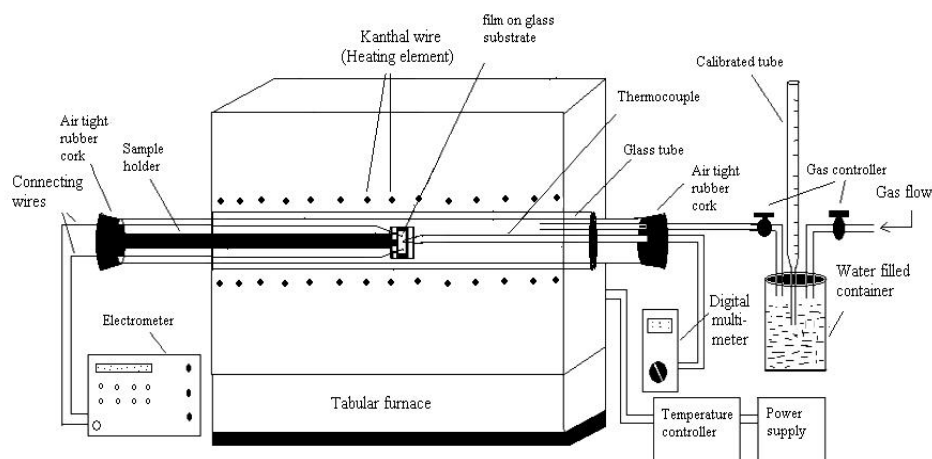

Fig. 1 − Schematic representation of gas sensor assembly and hydrogen volume measurement system

For making ohmic contacts at both the ends of the film, high conducting silver paste was used. The hydrogen sensing properties of the film was carried out in an indigenous gas sensor assembly shown in Fig. 1. The film was mounted on a home-made two-probe assembly placed into a silica tube which was inserted coaxially inside a resistance-heated furnace. The electrical resistance of the films was measured before and after exposure to hydrogen using a Keithley System Electrometer (Model: 6517B). The hydrogen volume measurement was done by water displacement method.

3. RESULTS AND DISCUSSION

Fig. 2 represents the XRD pattern of the film which is found to be polycrystalline zinc oxide in nature, possessing hexagonal wurtzite structure with preferred (002) orientation along the c-axis perpendicular to the substrate surface.
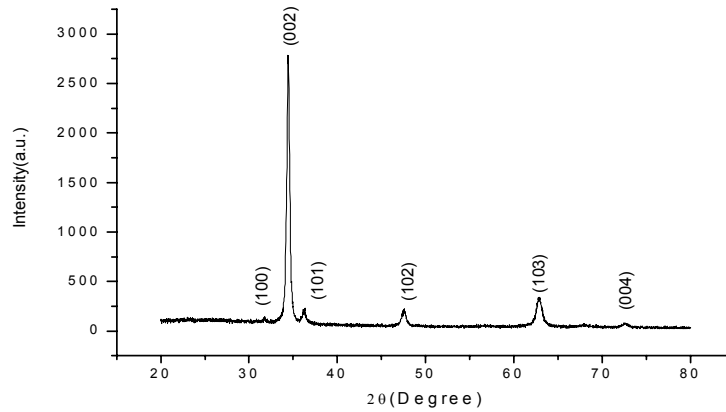

Fig. 2 − XRD spectra of the ZnO *film*

Other peaks corresponding to (100), (101), (102), (103) and (004) planes are present with low relative intensities (< 10%). The observed XRD pattern is found to match with JCPDS card (zinc oxide, 80-0074).
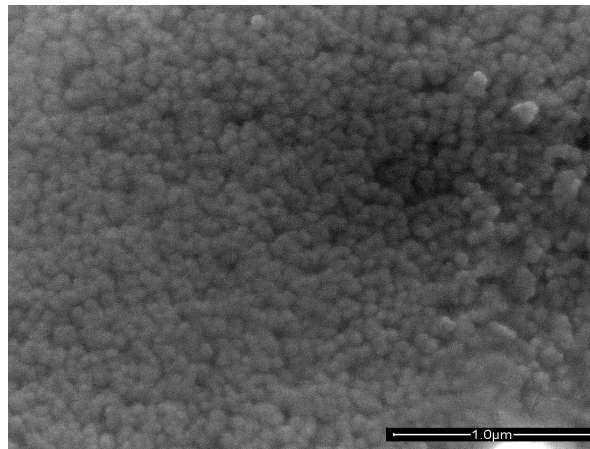

Fig. 3 − SEM image of the ZnO *film*

The average crystallite size (D) of the films is determined by using Scherrer formula [13]:

$$D = 0.9\lambda/\beta\cos\theta, \tag{1}$$

where λ, β and θ are the X-ray wavelength, full width at half maximum (FWHM) of the diffraction peak and the Bragg's diffraction angle, respectively. The lattice strain (ε) is determined using the tangent formula [13]:

$$\varepsilon = \beta/(4 \tan\theta), \tag{2}$$

The film is found to be nanocrystallites of grain size ~ 30-35 nm, having lattice strain 0.3689. Fig. 3 represents the SEM micrograph of the ZO1 film which shows the uniform polycrystalline surface having spherical- shaped grains, and no visible holes or faulty zones on the film surface are seen.
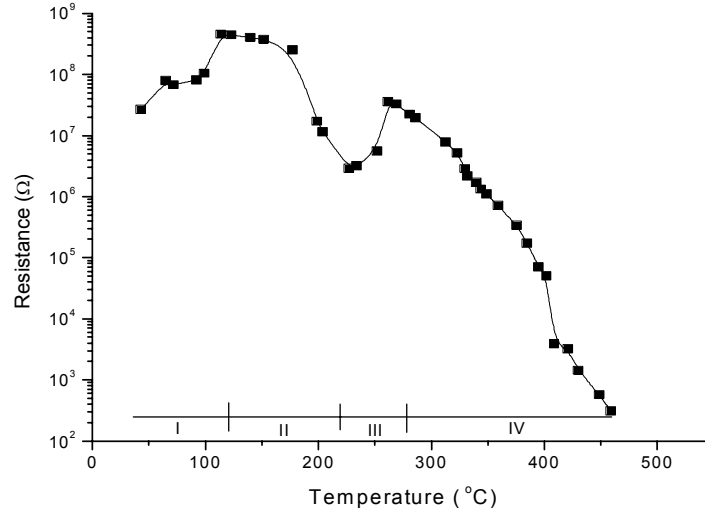

Fig. 4 − Electrical resistance of the ZnO *film as a function of temperature*

Fig. 4 represents the electrical resistance of the film as a function of operating temperature. It is observed that the resistance of the film first increases with temperature up to about 115 ºC (region I) which is attributed to the adsorption of atmospheric oxygen on the film surface. In region II, the decrease in resistance is attributed to the thermal excitation of electrons into the conduction band. The increase in resistance in region III is related to the dominant oxygen adsorption on the film surface; while the resistance in temperature range 260-460 ºC (region IV) decreases again, probably due to the dominant thermal excitation of electrons and the desorption of oxygen species.

As the film resistance decreases upon exposure to hydrogen, the sensor response is defined as $[((Ra - Rg)/Ra) \times 100\%]$. Here, Ra is the resistance of the film in air and Rg is the resistance upon exposure to hydrogen. Fig. 5 represents the sensing characteristics of the ZnO film as a function of operating temperatures for different volume concentrations of hydrogen in air. At low operating temperatures, the response of the film to hydrogen is restricted by the speed of the chemical reaction because the gas molecules do not possess sufficient thermal energy to react with the surface adsorbed oxygen species.

The response is found to be maximum (44.3 %) at the operating of tempera-ture of 250 °C for 0.8 vol.% concentration of hydrogen in air. In general, there exists an optimum working temperature of a sensor to achieve the maximum sensitivity to a gas of interest, the temperature being dependent upon the kind of gases, i.e., the mechanism of dissociation and further chemisorptions of a gas on the particular sensor surface.
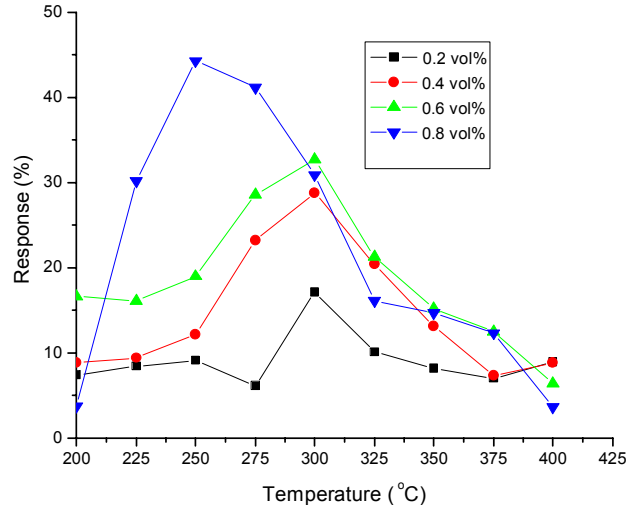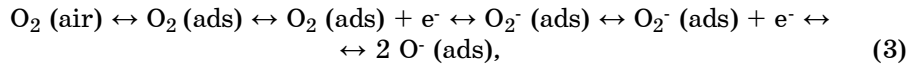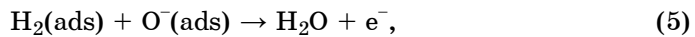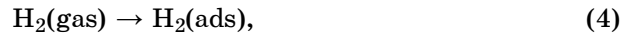
Fig. 5 − *Sensing characteristics of the* ZnO *film as a function of operating temperatures for various concentrations of hydrogen in air*

Fig. 6 represents the sensing characteristics of the ZnO film as a function of hydrogen gas concentration in air at operating temperatures of 250 °C and 300 °C for which the response is found to be maximum. At 250 °C, the response increases rapidly with increase in gas concentration because of much larger surface coverage of the gas molecules on the film surface and sufficient availability of adsorbed oxygen species on the sensing sites. However, at 300 °C, there is a gradual increase in sensor response after 0.4 vol.% gas concentration, implying that film surface begins to attain saturation in respect of gas reactivity. On increase in gas concentration after 0.6 vol%, the film shows a gradual decline in sensor response due to non-availability of sensing sites responsible for reaction to gas species. For all concentrations, the films show fast response and recovery at higher operating temperatures.

It is well known that in the temperature range between 100 and 500 °C oxygen chemisorbs on the ZnO surface in a molecular (O_2^-) and atomic form (O^-). Since O_2^- has lower activation energy, it is dominating at temperatures below 200 °C and at higher temperatures, the O^- form dominates.

$$O_2 \text{ (air)} \leftrightarrow O_2 \text{ (ads)} \leftrightarrow O_2 \text{ (ads)} + e^- \leftrightarrow O_2^- \text{ (ads)} \leftrightarrow O_2^- \text{ (ads)} + e^- \leftrightarrow \\ \leftrightarrow 2\ O^- \text{ (ads)}, \qquad (3)$$

The reaction kinetics is as follows [14, 15]. When the ZnO film is exposed to hydrogen gas, its atoms react with chemisorbed oxygen ions and produce H_2O molecules consuming chemisorbed oxygen from the film surface by releasing electrons. The sensing mechanism for H_2 may be represented by the following reaction [16, 17],
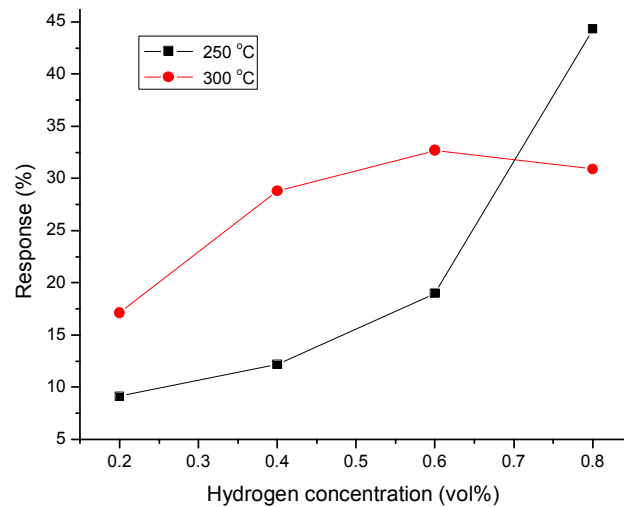
$$H_2\text{(gas)} \rightarrow H_2\text{(ads)}, \qquad (4)$$

$$H_2\text{(ads)} + O^-\text{(ads)} \rightarrow H_2O + e^-, \qquad (5)$$

Fig. 6 *– Sensing characteristics of the* ZnO *film as a function of hydrogen concentration in air at operating temperatures of* 250 °C *and* 300 °C

Thus, electrons are released into the conduction band, thereby decreasing the resistance of the film upon exposure to hydrogen. The transient response characteristics of the film at the operating temperature of 250 °C for different hydrogen concentrations is shown in Fig. 7. It is observed that the response time increases with concentration because of large surface coverage of hydrogen molecules on the film. For 0.2 vol.% concentration, the film shows almost equal recovery and response times; while for other concentrations, the recovery time is found to be more as compared to the response time.
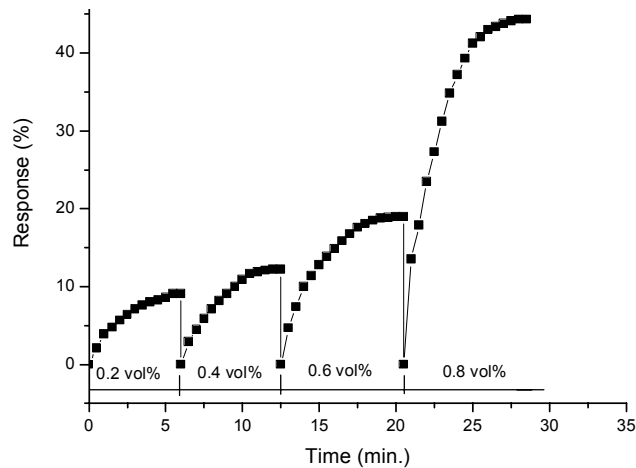

Fig. 7 *– Transient response characteristics of the film at the operating temperature of* 250 °C *for different hydrogen concentrations*

4. CONCLUSION

The ZnO thin films prepared by the pyrolytic decomposition of an aqueous solution of zinc nitrate are found to have hexagonal wurtzite nanostructure, having crystallite size in the range of 30-35 nm. The change in the film resistance as a function of operating temperature has been explained by three basic mechanisms: oxygen adsorption, electron excitation and oxygen desorption. The response of the film to hydrogen is observed to be maximum (44.3 %) at the operating of temperature of 250 °C for 0.8 vol.% concentration of hydrogen in air. Maximum response is attributed to the availability of sufficient adsorbed ionic species of oxygen on the film surface which react most effectively with H_2 molecules at this particular temperature. The reaction kinetics of H_2 gas sensing has been explained.

ACKNOWLEDGEMENTS

REFERENCES

1. M.A. Martнnez, J. Herrero, M.T. Gutiйrrez, *Solar Energ. Mater. Sol. C.* **45, 75** (1997).
2. S. Gledhill, A. Grimm, N. Allsop, T. Koehler, C. Camus, M. Lux-Steiner, C.-H. Fischer, *Thin Solid Films* **517, 2309** (2009).
3. K. Matsubara, P. Fons, K. Iwata, A. Yamada, K. Sakurai, H. Tampo, S. Niki, *Thin Solid Films* **431-432, 369** (2003).
4. J.-B. Lee, H.-J. Lee, S.-H. Seo, J.-S. Park, *Thin Solid Films* **398-399, 641** (2001).
5. L. Gong, Z. Ye, J. Lu, L. Zhu, J. Huang, X. Gu, B. Zhao, *Vacuum* **84, 947** (2010).
6. S.T. Shishiyanu, T.S. Shishiyanu, O.I. Lupan, *Sens. Actuat. B-Chem.* **107, 379** (2005).
7. M. Suchea, S. Christoulakis, K. Moschovis, N. Katsarakis, G. Kiriakidis, *Thin Solid Films* **515, 551** (2006).
8. P.P. Sahay, *J. Mater. Sci.* **40, 4383** (2005).
9. P.P. Sahay, S. Tewari, S. Jha, M. Shamsuddin, *J. Mater. Sci.* **40, 4791** (2005).
10. Y. Hu, X. Zhou, Q. Han, Q. Cao, Y. Huang, *Mater. Sci. Eng. B* **99, 41** (2003).
11. Q. Xiang, G. Meng, Y. Zhang, J. Xu, P. Xu, Q. Pan, W. Yu, *Sens. Actuat. B-Chem.* **143, 635** (2010).
12. C.S. Prajapati, S.N. Pandey, P.P. Sahay, *Physica B* **406**, 2684 (2011).
13. H.P. Klug, L.E. Alexander, *X-Ray Diffraction Procedures for Polycrystalline and Amorphous Materials* (Wiley Publishing: 1974).
14. K. Arshak, I. Gaiden, *Mater. Sci. Eng. B* **118, 44** (2005).
15. P.P. Sahay, R.K. Nath, *Sens. Actuat. B-Chem.* **133, 222** (2008).
16. O. Lupan, G. Chai, L. Chow, *Microelectron. Eng. B* **85, 2220** (2008).
17. O. Lupan, V.V. Ursaki, G. Chai, L. Chow, G.A. Emelchenko, I.M. Tiginyanu, A.N. Gruzintsev, A.N. Redkin, *Sens. Actuat. B-Chem.* **144, 56** (2010).